Advanced Materials '93, VI / Frontiers in
Materials Science and Engineering, edited by S. Sōmiya et al.
Trans. Mat. Res. Soc. Jpn., Volume 19B
1994 Elsevier Science B.V.

Better ceramics through metal modification

Jürgen Rödel, Helge Prielipp, Mathias Knechtel and Nils Claussen

Advanced Ceramics Group, Technische Universität Hamburg-Harburg,
21071 Hamburg, Germany #

The mechanical properties of metal reinforced ceramics, especially Al/Al_2O_3 and Cu/Al_2O_3 composites with interpenetrating networks, are described. Key parameters to tailor the characteristics of these materials are ligament diameter and volume fraction of the ductile reinforcement as well as fracture energy of the metal/ceramic interface. Data for fracture strength and fracture toughness are given as a function of all three variables and qualitative descriptions are provided for trends observed in the experiments. Finally, drastic improvements in thermal shock resistance of Al/Al_2O_3 composites with increasing ligament diameter highlight the opportunities afforded by tailoring the microstructure of metal reinforced ceramics.

1. Introduction

Metal modified ceramics have very attractive mechanical properties when designed as interpenetrating networks. In this case, the stiffness is provided by the ceramic network, the prospective failure site is defined by the ceramic network and failure will be governed by laws as applicable for ceramics. Specifically, plastic yielding as in a metal - dominated composite will not result in premature loss of tensile strength. Fracture toughness, on the other hand, will be mainly governed by the properties of the ductile reinforcement. The surrounding ceramic will help in hindering extensive plastic deformation, which will lead to an increase in uniaxial stress the metal can sustain before yielding. The degree of ductile deformation will therefore depend on the interfacial properties between metal and ceramic, but also on the detailed geometry of the reinforcing phase. Finally, an increase in toughness, invoked by the metal network, will lead to an increase in strength of the composite beyond values of the monolithic ceramic.

A substantial body of work, both in the field of ceramics [1-5] and in that of intermetallics [6-9] contributes to our current understanding. The ensuing research centered on the realization that crack bridging with attendant closure forces across the crack faces [10,11] can

This work was funded in part by DFG under contract number Ro: 954/1-1 and the Volkswagen Foundation under contract number 1/666 790.

be utilized in a more general manner than process zone shielding [12] in order to toughen ceramics. Furthermore, the production of ceramic matrix materials via directed metal oxidation [13] allows large scale manufacture of ductile phase reinforced ceramics. Vital precedents of ductile phase toughening can be drawn on in the work on cemented carbides, stemming largely from research performed in the late 70s [14,15], but also late 80s [16-18]. A second, seemingly independent line came from an interest in ductile phase toughening in glasses [19] , where also crack bridging arguments were developed [20].

It is now well appreciated that ceramic matrix composites reinforced by ductile phases can offer properties such as high hardness and wear resistance (based predominantly on the ceramic constituent), high fracture toughness , K_{Ic} (as in WC/Co with a value of 15 MPa·$m^{1/2}$) [16], high fracture strength, σ_f (as in Al/Al_2O_3 with a value of 760 MPa) [21] and high Weibull modulus, m (as in Zr/ZrB_2/ZrC with m = 68) [22].

The intent of this paper is to provide a perspective for the range of mechanical properties which can be achieved with metal reinforced ceramics. Three key parameters in tailoring the characteristics of these composites are investigated; metal ligament diameter, metal volume fraction and fracture resistance of the metal/ceramic interface. Finally, recent results on thermal shock resistance of Al/Al_2O_3 composites are presented.

2. Fracture Mechanics

Possible reinforcement mechanisms are depicted in Fig. 1. Ductile phases as well as grains, whiskers, platelets or fibers can reinforce a ceramic matrix by providing closure forces in the crack wake shielding the crack tip from the applied stress.

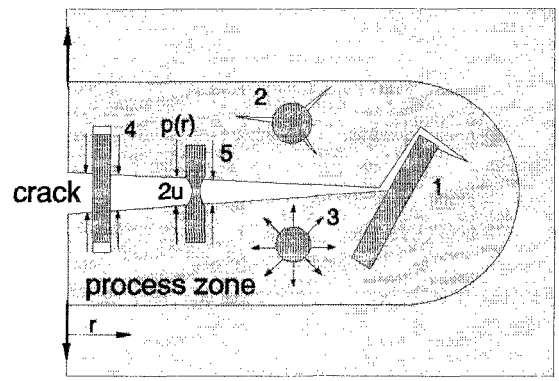

Figure 1: Schematic shows possible reinforcement mechanisms for ceramic matrix including crack deflection (1), microcrack toughening (2), transformation toughening (3), crack bridging by grains, whiskers, platelets or fibers (4) and crack bridging by ductile phases (5).

In a stress intensity factor notation, the equilibrium crack configuration with an applied stress intensity factor K_A, a crack length (c) dependent fracture toughness $K_R(c)$ can be written as (Eq. 1):

$$K_A = T_\mu(c) + T_0 = K_R(c) \qquad (1)$$

The fracture toughness is seen as being composed of a crack tip toughness term, T_0, and a microstructural term $T_\mu(c)$,

which sums up the closure stresses p(r) of all reinforcements and can be described by Eq. (2), where a weight function, g(c,r), appropriate for the respective crack configuration, has to be included.

$$T_\mu(c) = \int_0^c g(c,r)\, p(r)\, dr \qquad (2)$$

While the underlying description in Eq. (2) appears very informative, it is not fundamental, since in detail the closure stresses p(r) are a function of the crack opening displacement (COD), 2u, and will therefore change with crack length (which will affect the local COD). The notation of mechanical energy release rates, G, which implicitly includes closure stresses as a function of COD, may therefore be more insightful. The crack resistance term, R(c), is written then as a sum of a crack tip resistance, R_0, and a microstructural term, R_μ, which, again in equilibrium, is balanced by G (Eq. 3).

$$G = R_0 + R_\mu = R(c) \qquad (3)$$

R_μ can be found, using the J - integral formalism [23] (Eq. 4), where u_b is the opening at the last active bridge:

$$R_\mu = 2\, f \int_0^{u_b} p(u)\, du \qquad (4)$$

description is given here. Three materials with different microstructural scale (termed small (s), medium (m) and coarse (c)) were produced. An alumina with small pore channels was manufactured using the

There is general agreement that the toughening contribution by plastic deformation of the ductile phases is governed by the yield strength of the metal constituent, its area fraction f, and its uniaxial flow stress as established under the constraint of the more or less well bonded interface between metal and brittle matrix. The change of uniaxial stress, p, in the bridging ligament with crack opening, 2u, is represented by a stress displacement function, p(u), which uniquely describes the reinforcement characteristic [24] and is responsible for the increasing fracture resistance with crack length R(c).

In the elastic case or elastic-plastic case under small scale yielding conditions, we can use the relation between stress intensity factor and mechanical energy release rate (with E' Young's modulus under plane strain conditions), (Eq. 5):

$$G_A = \frac{K_A^2}{E'} \qquad (5)$$

3. Processing and Characterization Techniques

Most materials discussed in this paper (except for Fig. 10 a,b) were prepared by gas pressure metal infiltration. This processing method is described in detail in a paper on mechanical properties of Al/Al_2O_3 composites with interpenetrating phase networks [25]. Only a brief description is given here. Three materials with different microstructural scale (termed small (s), medium (m) and coarse (c)) were produced. An alumina with small pore channels was manufactured using the

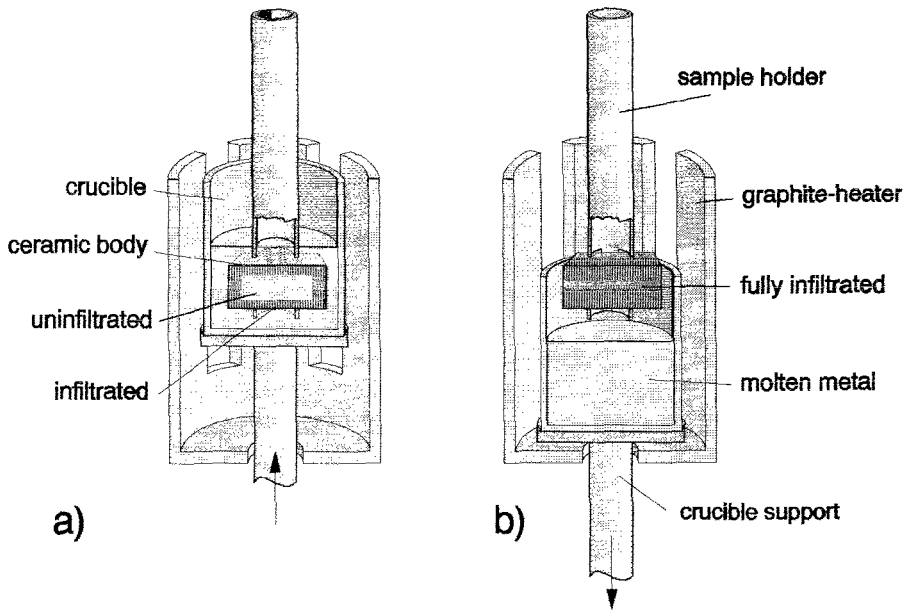

Figure 2: Schematic of gas pressure metal infiltration furnace during infiltration (a) and after infiltration (b).

RBAO process [26], starting with 55 vol.% Al and 45 vol.-% Al_2O_3. After a sequence of attrition milling, drying, breaking and sieving the powder mixture was uniaxially pressed into plates at 50 MPa and then cold isostatically pressed at 250 MPa. Densification at 1150 °C for 6 hours yielded a porous alumina with a density of 75 % TD. Medium sized metal channels resulted form a slip cast fine grained alumina powder, which was sintered with adjusted sintering schedules to yield densities of 60, 65 or 75 % TD, respectively. The third composite with coarse metal channels was based on a porous alumina, again with density of 75 % TD (for thermal shock testing 65 % TD), which was slip cast from an attrition milled (4 h at 300 rpm) coarse grained alumina powder and then sintered. All three porous aluminas exhibited a narrow distribution of the intrusion channel size as measured by mercury porosimetry. The corresponding value for a medium intrusion channel size was 0.08 μm, 0.23 μm and 0.97 μm for the small (s), medium (m) and coarse (c) scale materials, respectively. Porous plates of dimensions 52 x 38 x 10 mm were infiltrated with aluminum in a specially designed gas pressure metal infiltration furnace with incorporated hydraulic ram (Fig. 2). The plates were originally held in a fixture which was immersed in a crucible filled with metal chips. For aluminum (copper) the furnace was heated to 1050 °C (1350 °C) in vacuum, and an argon pressure of 15 MPa was applied for 30 min.

Subsequently, the furnace was cooled down and at 700 °C (1200 °C) the infiltrated plates were lifted out of the metal bath. Attained composites had a remaining porosity of about 1 %(2 - 8 %).

Fracture strength was measured in 4 pt. bending according to German standard DIN 51 110 but with rectangular bars of reduced length (25 x 4 x 3 mm) and loading spans of 10 and 20 mm. The tensile side was polished to a 3 μm surface finish and the edges were bevelled.

Fracture toughness was determined using the SEPB method (DIN 51 109) using five bars of same size as described above. Precracks were 1 to 2 mm long. Samples were renotched before testing to leave metal - ligament bridging lengths of less than 25 % of the total (including the notched) crack size.

Thermal quenching was performed from temperatures between 120 and 620 °C into water of 20 °C. Five samples were tested for each temperature difference.

Optical microscopy was used to characterize the microstructures obtained and scanning electron microscopy (SEM) to investigate the fracture surfaces. Observations from in situ SEM crack propagation studies are also provided [27].

4. Role of Metal Ligament Diameter

Representative micrographs of the medium grained and the coarse grained Al/Al_2O_3 composites are provided in Figs. 3 a and b, respectively. The intrusion pore sizes used to describe the three porous aluminas represents only bottle necks. Average ligament diameters as measured from polished sections give values which lie about a factor of 10 higher. Nevertheless, irrespective of parameter

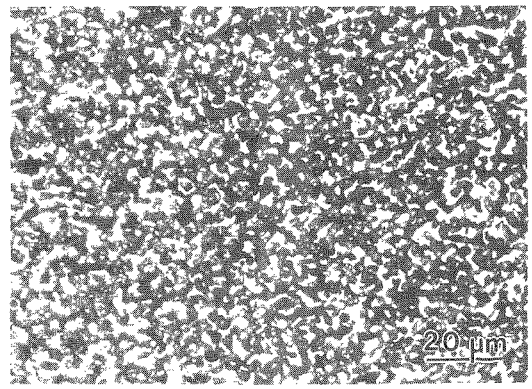

a)

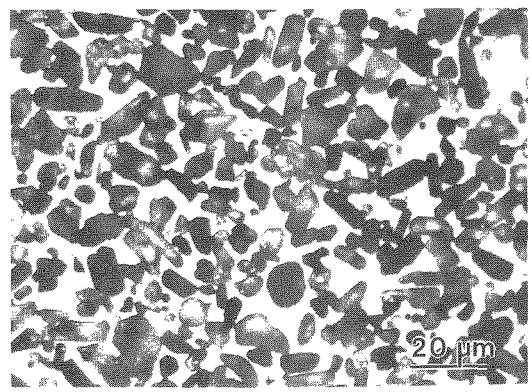

b)

Figure 3: Representative optical micrographs of medium grained (a) as well as coarse grained (b) Al/Al_2O_3 composites with 35 vol.-% Al.

used to characterize the scale, comparisons between different scale microstructures indicate a true scale invariance.

Fracture strength and fracture toughness values of the porous preforms as well as the Al/Al_2O_3 composites containing 25 vol.-% metal are given in Fig. 4 and 5. Aluminum infiltration

increases the fracture strength from values between 130 to 150 MPa for the porous preform to values between 540 to 680 for the composites. Similarly, fracture toughness increases from between 1.5 to 1.9 MPa·$m^{1/2}$ for the porous alumina to 2.9 to 7.4 MPa·$m^{1/2}$ for the metal reinforced ceramics. Again, observations on fracture surfaces of different scale microstructures point to a scale invariant metal deformation and debond lengths.

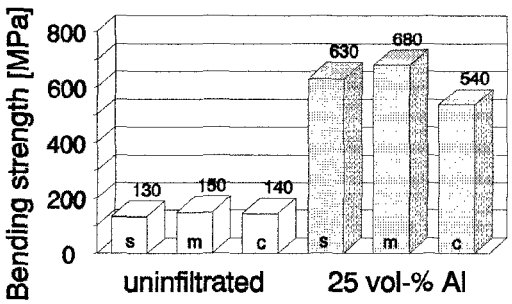

Figure 4: Fracture strength of Al/Al_2O_3 composites with 25 vol.-% metal and varying ligament diameter.

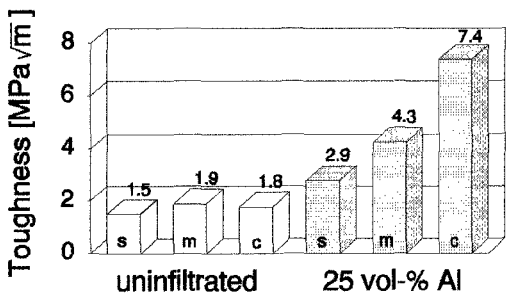

Figure 5: Fracture toughness of Al/Al_2O_3 composites with 25 vol.-% metal and varying ligament diameter compared to the corresponding values for the porous preforms.

Consecutively, p(u) functions can be derived which can be computed from one assumed function and simply be transformed into another microstructural scale by stretching the crack opening parameter in accordance with the ligament diameter (Fig. 6).

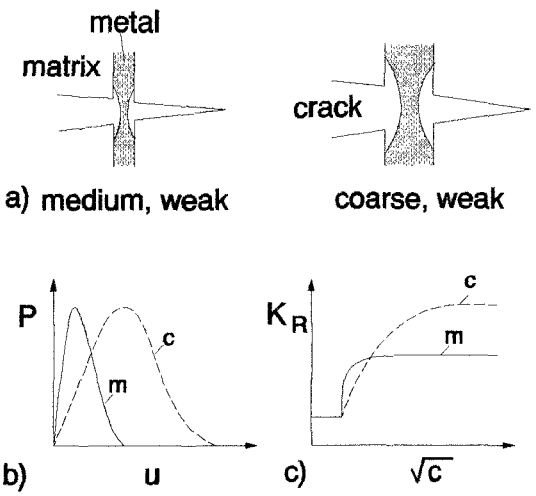

Figure 6: Schematic describing p(u) functions (b) and R-curves (c) for metal reinforced ceramics with varying ligament diameter (a), based on the assumption of scale independent metal deformation.

Large reinforcements will therefore lead to smaller crack closure stress at given COD, which, however will be maintained up to higher crack opening displacements. This will result in R - curves for the large reinforcement which can be characterized by a small, initial slope, but a high peak toughness. Therefore, long - crack fracture toughness (as measured by SEPB) will increase with ligament diameter. In describing fracture strength, the actual slope of the R-curve, as well as the initial flaw size, come critically into play. In our

case, the large grained composite appears to exhibit too shallow an R-curve so that crack instability occurs with a small degree of stable crack growth and, therefore, at a small toughness increment, which leads to a comparatively low strength. The fine grained micostructure exhibits only a very small R-curve altogether, so that the increase in strength is not as dramatic. Conversely, the medium scale microstructure appears to combine initial flaw size and slope of the R-curve most favorably and therefore has the highest fracture strength of 680 MPa. Due attention has to be paid to the scale of the initial flaw size. In cases where this parameter is increased (as in thermal shock, see chapter 7), the large scale microstructure may prove to be advantageous compared to the fine or medium scale counterparts.

Finally, the strength distributions for the three composites (Fig. 7b) are compared with corresponding results of the porous preforms (Fig. 7a). The porous aluminas exhibited a Weibull modulus of 6 - 12, while for the composites, it varies with increasing scale from 10 to 12 and then 19. This trend can be understood by appreciating again the relative scale of initial flaw size and degree of stable crack growth. Larger initial flaws can lead to a larger degree of stable crack growth, which can provide a rather large toughness increase. This is only true, if the R-curve is of sufficiently large scale. While these arguments are only qualitative, they may suffice at this juncture to provide some fundamental insight into the reinforcement mechanism originating from ductile ligaments. It should also be pointed out that qualitative descriptions of the effects of R-curve behavior on reliability are available in the literature [28-30].

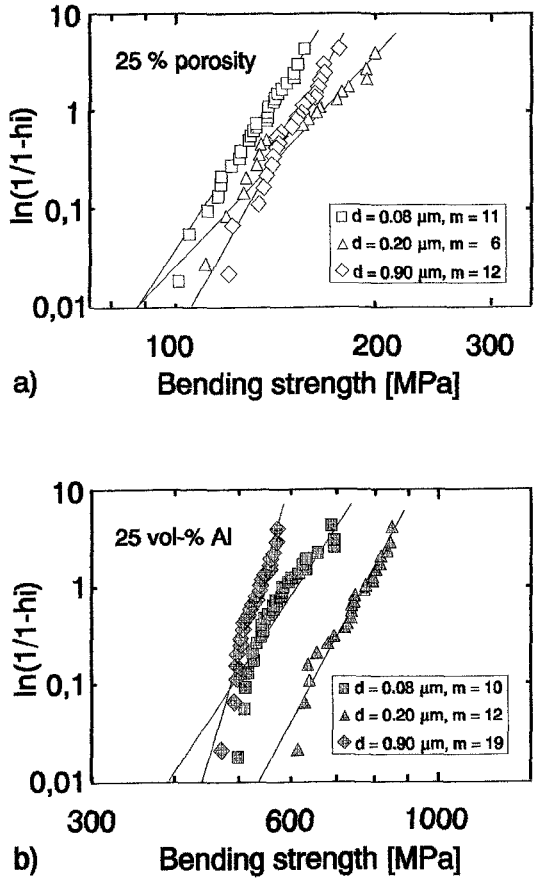

Figure 7: Strength distribution for preforms with 75 % TD for different microstructural scale (a) and of Al/Al_2O_3 composites with 25 vol.-% metal and varying ligament diameter.

5. Role of Metal Content

The influence of metal content was simply studied by partially sintering alumina preforms made from the medium scale powder to various densities and then

infiltrating the pore space with aluminum. The results of fracture strength versus volume fraction Al (Fig. 8) can be compared with tensile strength data for Al_2O_3 dispersion strengthened aluminum [31]. An improvement in fracture strength with increasing metal content is observed. The highest strength value (855 MPa) was found for the composite with 40 vol.-% metal. Fracture toughness increases from 4.3 MPa·$m^{1/2}$ to 6.1 MPa·$m^{1/2}$ if the content of aluminum is increased from 25 to 35 vol. %. Again, the trends in toughness are easily rationalized by employing Eq. 4, where an increase in area fraction of the reinforcing phase will lead to an increase in fracture toughness. A quantitative measure of this increase would have to include a change in average pore channel size with density and has not been obtained yet.

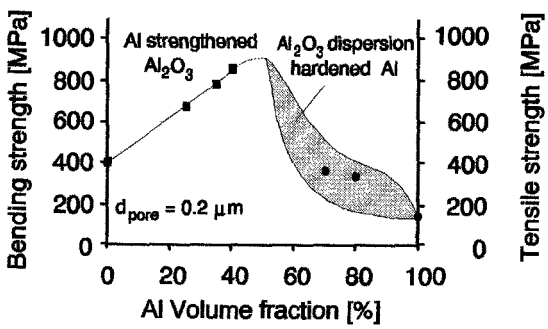

Figure 8: Fracture strength of Al/Al_2O_3 composites with medium ligament diameter and varying metal content as compared to dispersion strengthened aluminum.

The increase in fracture strength with metal content may seem surprising at first, since aluminum has a strength much below the strength of alumina, so clearly, any rules of mixing do not apply. To understand the strength of metal/ceramic composites one needs to appreciate that, in interconnecting networks, the ceramic provides the failure site at the largest flaw and the metal provides the fracture toughness. An increase in metal content results from a preform with high porosity and therefore with a large initial flaw (Fig. 9).

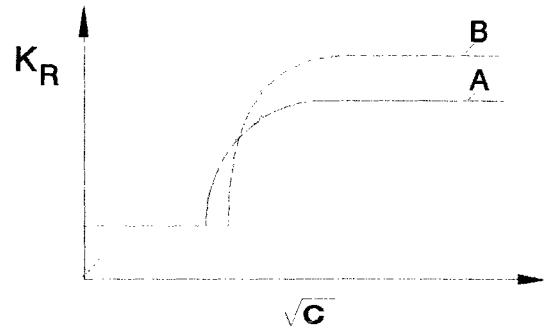

Figure 9: Schematic describing R-curves of metal reinforced ceramics with varying metal content (A: small metal content, B: high metal content). The tangency condition of the applied stress intensity factor (straight, dashed lines) with the R - curves yields the respective instability points.

Depending on exact interaction of initial pore size and slope of R-curve, an increase or decrease of strength with metal content may result. In the case of aluminum reinforcement, the R-curves are steep enough to compensate for the increase in initial flaw size and therefore yield an increase in strength (tangency condition in Fig. 9) with increasing metal content.

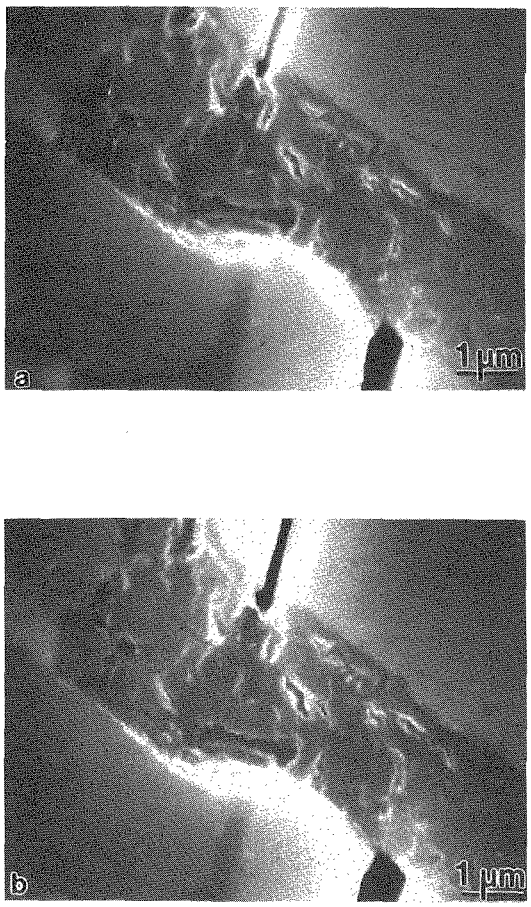

Figure 10: Surface view of Al ligament in a material prepared by directed metal oxidation showing plastic deformation through hole nucleation and hole growth with region 360 μm (a) and 400 μm (b) behind crack tip [27].

6. Role of Interfacial Fracture Resistance

The influence of interfacial fracture resistance was studied by contrasting the mechanical behavior of Al/Al_2O_3 composites with Cu/Al_2O_3 composites. The aluminum/alumina interface is generally described as a "strong" interface [32], while the copper/alumina interface, at low oxygen partial pressure, has been described as a "weak" interface [33]. Although the stress - strain curves of pure copper and pure aluminum are also different, the determining factor for differences in the mechanical behavior of either aluminum or copper reinforced alumina is expected to be derived rather from the interface than the bulk metal properties.

In situ observations during crack propagation in the SEM [27] can give insight into the deformation mechanism of the metal ligament. In Fig. 10 a and b, an aluminum ligament in a material prepared by directed metal oxidation (containing aluminum, silicon, alumina and silicon carbide) [27] is shown at different applied loads and crack lengths. A strong interface leads to only limited debonding and is responsible for a state of hydrostatic stress in the metal. Failure occurs finally through hole nucleation (Fig. 10 a) and hole growth (Fig. 10b). Fig. 11 a and b compares fracture surfaces of Al/Al_2O_3 composites with Cu/Al_2O_3 composites, both containing 35 vol.-% metal with medium ligament diameter. Again, only little debonding is visible at aluminum/alumina interfaces, some cavitation and predominantly transgranular fracture of the ceramic. In contrast, copper/alumina interfaces exhibit a large degree of debonding and intergranular fracture of the alumina. A low interfacial fracture resistance leads to unconstrained metal deformation associated with low

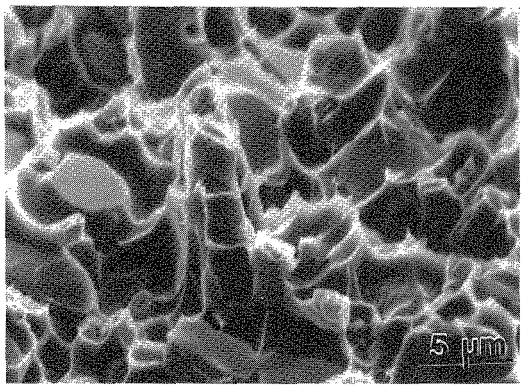

a)

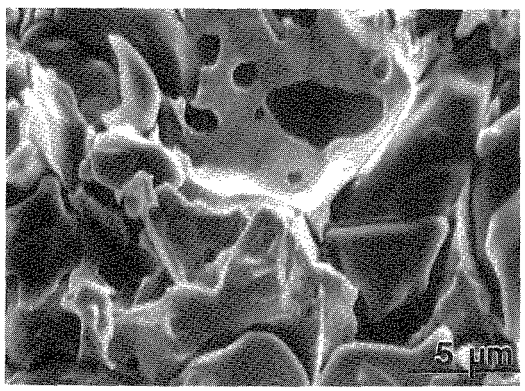

b)

Figure 11: Fracture surfaces of Al/Al_2O_3 composites (a) and Cu/Al_2O_3 composites (b) with 35 vol.-% metal of medium ligament diameter.

closure stresses at small COD and should therefore result in low strength values for the Cu/Al_2O_3 composite verified in Table 1. The fracture toughness of the copper reinforced alumina is low as compared with the aluminum reinforced ceramic, presumably due to the low ductility of copper.

Table 1: Fracture strength and fracture toughness of Al/Al_2O_3 composites (a) and Cu/Al_2O_3 composites (b) with 35 vol.-% metal and medium ligament diameter.

	Strength [MPa]	Toughness [MPa$\sqrt{m}$]
Al	655 +/- 64	10,4 +/- 0,7
Cu	218 +/- 27	6,3 +/- 0,2

P(u) functions and R-curves are contrasted in Fig. 12 for the cases of "weak" and "strong" interfaces. The latter will result in high closure stresses at small COD, hence in a steep R-curve at small degrees of crack extension, which in turn will result in high strength values.

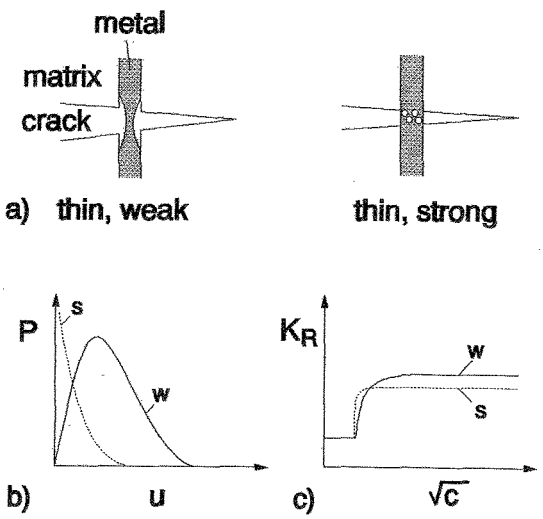

Figure 12: Schematic describing p(u) functions (b) and R-curves (c) for "weak" vs. "strong" interfaces (a).

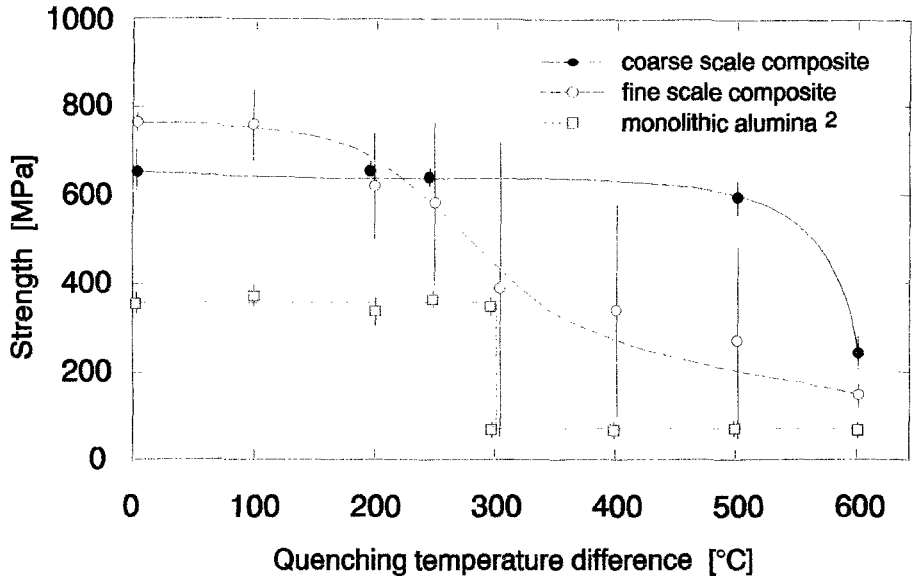

Figure 13: Retained fracture strength for medium scale (open circles) and coarse scale (full circle) Al/Al_2O_3 composites compared to that for monolithic alumina (open squares ([34]).

7. Thermal Shock Resistance

Thermal shock strength data of two Al/Al_2O_3 composites with 35 vol.-% metal content and either medium or coarse ligament diameter are compared in Fig. 13 with literature data of a monolithic alumina tested in the form of rods with a diameter of 4.7 mm [34]. The composite with the medium grained alumina shows a gradual decrease in retained strength over an interval of 100 °C < ΔT < 400 °C but remains stronger than the monolithic alumina at all quenching temperature differences investigated. The decrease in retained strength for the medium scale composite continues even above ΔT = 400 °C. At ΔT = 600 °C, however, the retained strength is still at 150 MPa, which is to be compared to the corresponding value of the monolithic alumina (70 MPa). The coarse grained Al/Al_2O_3 composite retains more than 90 % (600 MPa) of its initial strength even at ΔT = 500 °C and only then shows a significant decrease to 240 MPa at ΔT = 600 °C.

The key to the results given in Fig. 13 lies in a balance between crack driving force due to transient stress fields and R-curve associated with metal reinforcement [35]. R-curve behavior will lead to stable crack growth during thermal quenching and will thereby smear out the otherwise sharp critical quenching temperature difference, ΔT_c, at which a strong drop in retained strength occurs. An increase in crack length during thermal shock treatment is furthermore buffered by an

increase in fracture toughness, which ideally leads to only a small decrease in retained strength. Most dramatic, however, is the increase in thermal shock resistance with increasing ligament size. This is explained by a large degree of stable crack propagation and by the avoidance of unstable crack propagation, thereby retaining small flaw sizes accompanied with relatively high fracture toughness values.

8. Conclusions

Metal reinforced ceramics, particularly when designed as interconnecting phase networks, may attain high strength, high toughness and high reliability. Through the influence of ligament size, metal content and interfacial fracture toughness on mechanical properties of these composites, a large degree of freedom is available to produce materials with tailored mechanical properties. Beyond their applicability as technical ceramics, metal/ceramic materials can also be used as model microstructures to study and understand the influence of R-curve behavior on reliability, thermal shock behavior etc.

REFERENCES

1. L.S. Sigl, P.A. Mataga, B.J. Dalgleish, R.M. McMeeking, and A.G. Evans, Acta metall., **36** [4] 945-953 (1988).
2. B.D. Flinn, M. Rühle, and A.G. Evans, Acta metall., **37** [11] 3001-3006 (1989).
3. M.F. Ashby, F.J. Blunt, and M. Bannister, Acta metall. mater., **37** [7] 1847-1857 (1989).
4. P.A. Mataga, Acta metall., **37** [12] 3349-3359 (1989).
5. G. Bao and C. -Y. Hui, Int. J. Sol. Struct., **26** [5/6] 631-642 (1990).
6. H.C. Cao, B.J. Dalgleish, H.E. Deve, C. Elliott, A.G. Evans, R. Mehrabian, and G.R. Odette, Acta metall., **37** [11] 2969-2977 (1989).
7. H.E. Deve, A.G. Evans, G.R. Odette, R. Mehrabian, M.L. Emiliani, and R.J. Hecht, Acta metall., **38** [8] 1491-1502 (1990).
8. T.C. Lu, A.G. Evans, R.J. Hecht, and R. Mehrabian, Acta metall. mater., **39** 1853-1862 (1991).
9. L. Xiao and R. Abbaschian, Mat. Sci. and Eng., **A155**, 135-145 (1992).
10. R. Knehans and R. Steinbrech, J. Mat. Sci. Lett. 1, 327-329 (1982).
11. P.L. Swanson, C.J. Fairbanks, B.R. Lawn, Y.-W. Mai, and B. J. Hockey, J. Am. Ceram. Soc., **70** [4] 279-289 (1987).
12. A.G. Evans and R.M. Cannon, Acta metall., **34** [5] 761-800 (1986).

13a. M.S. Newkirk, A.W. Urquhart, H.R. Zwicker and E. Breval, J. Mater. Res. **1** [1] 81-89 (1986).

13b. N. Claussen and A.W. Urquhart, Encyclopedia of Materials and Engineering, Suppl. Vol. 2, ed. R.W. Cahn, Pergamon Press, Oxford, U.K. (1990).

14. A.G. Evans, A.H. Heuer, and D.L. Porter, pp. 529-556 in Proc. of the 4th. Int. Conf. on Fracture, ed.

D.M.R. Taplin, Pergamon Press, New York, (1977).
15. M. Nakamura and J. Gurland, Metall. Trans, **11A**, 141-146 (1980).
16. L.S. Sigl, Fortschrittberichte VDI, Reihe 5, Nr. 104.
17. L.S. Sigl and H.E. Exner, Met. Trans., A, **18A** 1299-1308 (1987).
18. L.S. Sigl and H.F. Fischmeister, Acta metall., **36** [4] 887-897 (1988).
19. V.V. Krstic, P.S. Nicholson, and R.G. Hoagland, J. Am. Ceram. Soc., **64** [9] 499-504 (1981).
20. V.D. Krstic, Philos Mag., **A48**, 695 (1983).
21. S. Wu, A.J. Gesing, N.A. Travitzky, and N. Claussen, J. Eur. Ceram. Soc., **7**, 277-281(1991).
22. T.D. Claar, W.B. Johnson, C.A. Anderson, and G.H. Schiroky, Ceram. Eng. Sci. Proc., **10** [7-8] 599-609 (1989).
23. J.R. Rice, J. Appl. Mech. **35**, 379-386 (1968).
24. A.G. Evans and R.M. McMeeking, Acta metall., **34** [12] 2435-2441 (1986).
25. H. Prielipp, M.C. Knechtel, J. Rödel and N. Claussen, submitted to J. Mat. Sci.
26a. N. Claussen, T. Le and S. Wu, J. Eur. Ceram. Soc., **5**, 29-35 (1989).
26b. S. Wu, D. Holz and N. Claussen, J. Am. Ceram. Soc., **76** [4] 970-980 (1993).
27. J. Rödel, M. Sindel, M. Dransmann, R. Steinbrech and N. Claussen, submitted to J. Eur. Ceram. Soc.
28. K. Kendall, N. McN. Alford, S.R. Tan and J.D. Birchall, J. Mater. Res. **1** [1] 120-123(1986).
29. R.F. Cook and D.R. Clarke, Acta metall., **36** [3] 555-562 (1988).
30. D.K. Shetty and J.S. Wang, J. Am. Ceram. Soc., **72** [7] 1158-1162 (1989).
31. F.A. Girot, J.M. Quenisset and R. Naslain, Comp. Sci. and Techn., **30**, 155-184 (1987).
32. B.J. Dalgleish, K.J. Trumble and A.G. Evans, "Acta metall., **37** [7] 1923-1931 (1989).
33. B. Gibbesch and G. Elssner, Acta metall. mater. **40** [S] S59-S66 (1992).
34. D.P.H. Hasselman, J. Am. Ceram. Soc., **52** [1] 600-604 (1969).
35. S. Schön, H. Prielipp, R. Janssen, J. Rödel and N. Claussen, submitted to J. Am. Ceram. Soc.

Claussen, Nils

Born on April 20, 1937, Hamburg, Germany

Nils Claussen is Professor and Head of Advanced Ceramics Group of the Technical University of Hamburg-Harburg (TUHH). After Earning his B.S.(1961) and M.S. (1963) in Mechanical Engineering from Stuttgart University, he obtained an M.S. in Metallurgy from Georgia Institute of Technology, Atlanta. In 1971, he received his Ph.D. in Chemical Engineering from Stuttgart University. From 1970 to 1985 he was Head of the Special Ceramics Group at Max-Planck-Institute of Metals Research in Stuttgart. In 1985 he joined the staff of TUHH in Hamburg.
Claussen is a Fellow of the American Ceramic Society (1982), member of the Academy of Ceramics (1989), honorary member of the Materials Research Society of Japan (1993), and member of several professional societies including the Ceramic Society of Japan. In 1978, he received the DECHEMA Award (German Chemical Engineering Society), in 1984 the Kraner Award of the American Ceramic Society, and in 1986 the G.W. Leibniz Award of the German Science Foundation. Claussen authored or coauthored more than 170 publications and owns 27 patents. He was Guest Scientist and Lecturer at the University of Valparaiso, Chile (1974), Shanghai Institute of Ceramics (1981), and CSIRO, Melbourne (1985 and 1991).